Evapotranspiration analysis based on topography algorithm in the Yellow River Delta

Jicai Ning[a], Zhiqiang Gao[*a,b], Runhe Shi[b],Wei Gao[b]

[a] Yantai Institute of Coastal Zone Research,

Chinese Academy of Sciences, Yantai, 264003 China;

[b] USDA UV-B Monitoring and Research Program, Natural Resource Ecology Laboratory, Colorado State University, Fort Collins, CO, USA

ABSTRACT

A remote sensing regional evapotranspiration (ET) model was built on the basis of topography correction (slope, aspect and elevation), herein. A variety of satellite data which have visible, near-infrared and thermal infrared remote sensing data can be used by this improved model. Combined with conventional ground meteorological information, it can estimate regional distribution of ET under different climate and terrain conditions, expanding the scope of application. Taking into account the terrain factors, we modified the algorithm of SEBAL model. Results showed that, the modified inversion method of evapotranspiration can better reflect actual evapotranspiration condition. Evapotranspiration changes were consistent with land use types. This research indicates that application of medium or high resolution satellite data to calculate regional ET under undulating landform should consider the impact of terrain. It improves the accuracy of ET estimates and has important reference value for the work of the regional water balance and regional agricultural climate research.

Key Words: Evapotranspiration(ET); SEBAL model; Landsat TM; Yellow River Delta

1. INTRODUCTION

Evapotranspiration is one of the most significant components of the hydrologic budget[1]. Quantifying the ET over large areas and within irrigated projects is important for water rights management, water resources planning, hydrologic water balances, and water regulation[2,3]. Conventional techniques that based on the point measurements are representative only of local scales and will fail for large scales. Satellite sensors that observe the earth from the space give a chance to estimate ET in a big scale. The accurate measurement of ET is of great significance for studying environmental sustainability, global climate changes, and biodiversity. Remote sensing technologies are capable of monitoring both energy and water fluxes on the surface of the Earth. With this advancement, existing models, such as SEBAL[4-6], SSEBI and SEBS, enable us to estimate the regional ET with limited temporal and spatial coverage in the study areas. Exchanges of materials and energy flows were more complex in the Yellow River Delta with the interaction between the land and the ocean[7]. Based on the widely and successfully applied SEBAL model, topography correction (slope, aspect and elevation) for some model parameters, automatically detection the dry and wet pixels and effectively simulated the evapotranspiration (ET) of the water body have been done to establish the regional ET remote sensing model in the context of digital elevation model (DEM), expanding the application of the regional ET remote sensing model. One of the weaknesses in SEBAL is the assumption of uniform, flat terrain. So, the objective of this paper is to couple the digital elevation model (DEM) into the SEBAL model for the topography correction (slope, aspect and elevation), expanding the application of the regional ET remote sensing model.

Address correspondence to * gaoland@gmail.com

Remote Sensing and Modeling of Ecosystems for Sustainability X, edited by Wei Gao, Thomas J. Jackson, Jinnian Wang, Ni-Bin Chang, Proc. of SPIE Vol. 8869, 88690G

2.Study area and material

The Yellow River Delta is located in Dongying City, Shandong Province, eastern China (Fig.1). Due to the low and flat terrain, high groundwater table, high mineralization rate, poor drainage conditions, infiltration and mounting of seawater associated with the water of the Yellow River, soil salinization in this area has been very severe. In this study, we used the Landsat5 TM image(path 121 row 034, acquired on 2 October 200). (Fig.2) All the bands of TM have the same resampling resolution of 30 ×30m. The corresponding weather data was acquired , including air temperature, wind and relative humidity at the same date as the RS image; Based on the remote sensing images, we can acquire the data of land use/coverage mainly by visual interpretation.

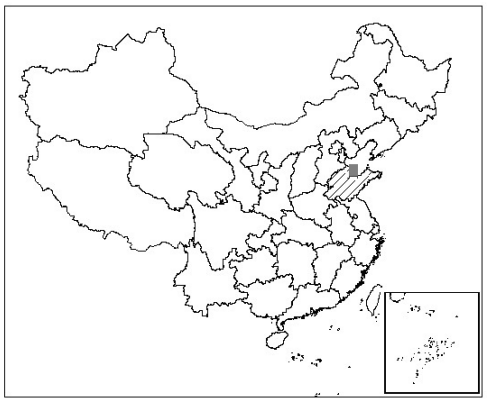

Figure 1. The location of study area

Figure 2. Landsat TM composite image of the study area(band 4, 3, 2)

3. METHODOLOGY

The theoretical and computational basis of SEBAL is described in Bastiaanssen et al. (1998), Bastiaanssen(2000), and Bastiaanssen et al.(2005). Although satellites routinely measure surface reflectance and some measure surface temperature, none measure near-surface vapor content. SEBAL computes a complete radiation and energy balance along with the resistances for momentum, heat and water vapour transport for each pixel. Evapotranspiration is derived in terms of instantaneous latent heat flux, λ ET (W m^{-2}), and it is computed as the residual of the surface energy balance equation at the moment of satellite overpass on a pixel-by-pixel basis:

$$\lambda ET = (Rn - G - H) \quad (1)$$

where Rn is net radiation (W/m^2), G is the soil heat flux (W/m^2), and H is the sensible heat flux (W/m^2).

The equation to calculate the net radiation is given by [8]

$$R_n = R_{s\downarrow} - \alpha R_{s\downarrow} + R_{L\downarrow} - R_{L\uparrow} - (1-\varepsilon_0)R_{L\downarrow} \quad (2)$$

where Rs ↓ is the incoming short-wave radiation [W/m^2], α is the surface albedo [-], RL ↓ is the incoming long wave radiation [W/m^2], RL ↑ is the outgoing long wave radiation [W/m2], and ε ois the surface thermal emissivity [-].

Soil heat flux G is evaluated by an empirical relation function by Bastiaanssen [13] with net radiation and a few other surface parameters, such as albedo, surface temperature and normalized difference vegetation index (NDVI):

$$G/R_n = T_s/\alpha(0.0038\alpha + 0.0074\alpha^2)(1 - 0.98\mathrm{NDVI}^4) \quad (3)$$

where Ts is surface temperature in K.

Sensible heat flux H is a function of the temperature gradient, surface roughness and wind speed and thus difficult to compute due to the interrelationship of temperature gradient and surface roughness. The classical expression for sensible heat flux is given by Farah and Bastiaanssen:

$$H = \rho C_p \frac{dT}{r_{ah}} \tag{4}$$

where ρ is the air density (kg m^{-3}) which is a function of atmospheric pressure, Cp is the specific heat capacity of air (≈1004 J kg^{-1} K^{-1}), dT is the near surface temperature difference (K), rah is the aerodynamic resistance to heat transport(s m^{-1}).

In the SEBAL model a linear relationship is introduced between the surface temperature Ts and dT to be calibrated on the basis of the knowledge of two boundary conditions identified within the image itself where the dT values can be backcalculated using a known H at the two pixels.

$$dT = aTs + b \tag{5}$$

The definition of a and b coefficients requires a choice of the two pixels, representing the extreme conditions of temperature and humidity, called the hot pixels and cold pixels. The cold pixel is a well-irrigated crop surface with full cover and the surface temperature (Ts) close to the air temperature (Ta). The hot pixel is a dry bare agricultural field where λET is assumed to be 0. The two pixels tie the calculations for all other pixels between these two points. An iterative way started from neutral stability assumptions is conducted for the sensible heat flux estimation using atmospheric stability corrections based on Monin－Obukhov.

Once the instantaneous latent heat flux, λET , is the calculated residual term of the energy budget, and it is then used to compute the instantaneous evaporative fraction Λ:

$$\Lambda = \frac{\lambda ET}{\lambda ET + H} = \frac{\lambda ET}{R_n - G_0} \tag{6}$$

The instantaneous evaporative fraction Λ expresses the ratio of the actual to the crop evaporative demand when the atmospheric moisture conditions are in equilibrium with the soil moisture conditions. Several studies [9] demonstrated that, within daytime hours, the Λ values are almost constant in time, thus allowing the use of as a temporal integration parameter. For timescales of 1 day or longer, G can be ignored and the net available energy (Rn － G) reduces to the net radiation (Rn). At daily timescales, ET24 (mm d^{-1}) can be computed as:

$$ET_{24} = \frac{86400 \times 10^3}{\lambda \rho_w} \Lambda R_{n24} \tag{7}$$

where: Rn24 (W m^{-2}) is the 24 h averaged net radiation, λ (J kg^{-1}) is the latent heat of vaporization, and ρ w (kg m^{-3}) is the density of water.

Internal calibration of the sensible heat computation within SEBAL model and the use of the indexed temperature gradient eliminate the need for refined atmospheric correction of surface temperature (Ts) or reflectance (albedo) measurements using radiative transfer models. The internal calibration also reduces impact of bias in estimation of aerodynamic stability correction or surface roughness. The attributes of the internal calibration and substantial compensation for component estimation biases enhance the operational applicability of the SEBAL model.

4. ANALYSIS AND RESULTS

The observation data were from the nearby station of Yucheng Ecological Experiment Observations. The retrieved value of evapotranspiration were close to the measured data. The relative error was less than 20%, which indicating that the modified SEBAL model was applicable to the study area.

4.1 Analysis of daily evapotranspiration

Evapotranspiration of the study area were ranged from 0.553 to 3.727 mm / d (Figure 3), with an

average of 2.98 mm / d. The maximum value of evapotranspiration appeared in the water body, while the minimum value occurs in area of saline and unused land which have sparse vegetation. It always has high evapotranspiration value in farmland areas for higher vegetation coverage.

Except for shrimp area mainly composed of water, the evapotranspiration value of the coastal area was always high for poor vegetation cover. In general, the evapotranspiration value increases with the distance from the coastline due to vegetation cover. Evapotranspiration of water body was usually higer than farmland, and that of farmland was higher than unused land because of water supply and vegetation cover rate.

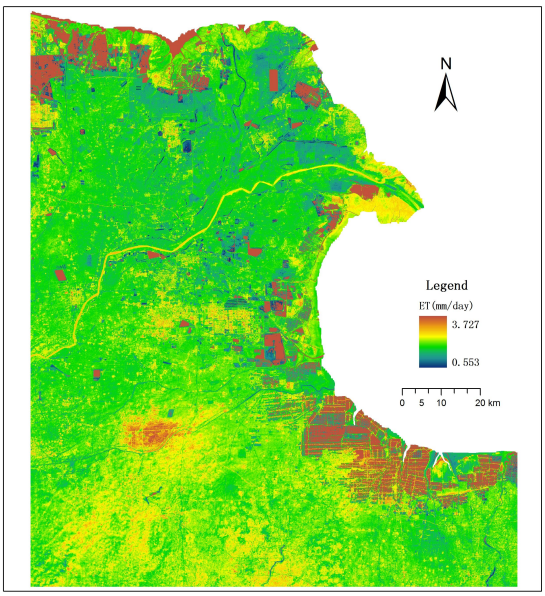

Figure 3. The distribution map of evapotranspiration

4.2 Analysis of daily evapotranspiration for different land use types

Accounting for land use type, the mean daily evapotranspiration of water bodies was the highest, with the value up to 3.31 mm / d, followed by arable land and grassland (2.81 mm / d and 2.56 mm / d respectively). The minimum value (less than 1.5 mm / d) happened in the residential area, salt land, and other unused land area.

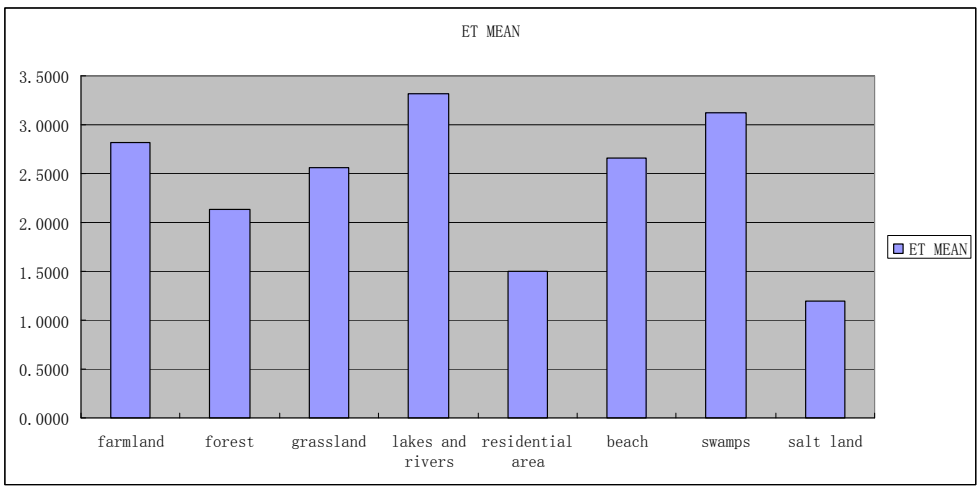

Figure 4. Mean value of daily evapotranspiration for different land use types

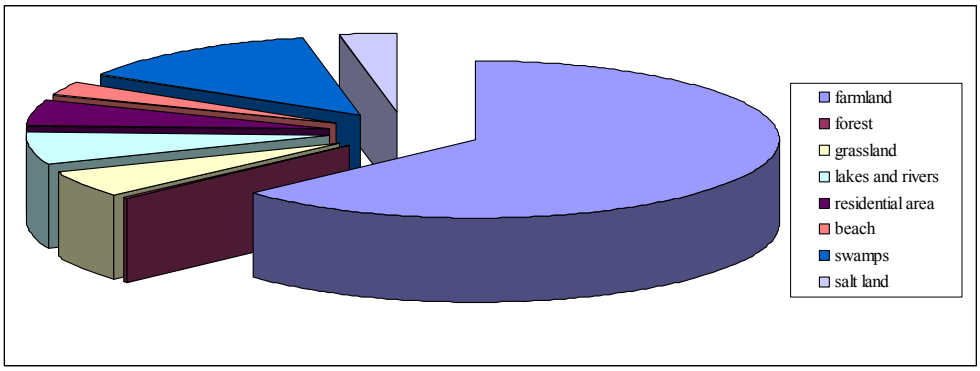

Figure 5. Proportion map of total daily evapotranspiration for different land use types

Taking into account the total amount, the evapotranspiration of farmland area accounted for 63.02%, followed by swamps area (accounted for 13.16%). On the other hand, the evapotranspiration of forests and salt land occupied the smallest percentage of total evapotranspiration(0.34% and 3.16% respectively). This is mainly related to different land use type's proportion. It is dominated by agricultural land in study area, and the crop evapotranspiration has the greatest impact.

4.3 Analysis of daily evapotranspiration for different landform types

It is generally composed by the plains and little hills in the study area, with the altitude ranging from -30m to 235m. The flat plains has the largest area, accounting for about 48.07 percent. Next to the flat plains is sloping plain, which accounting for about 26.18 percent. The area of high hills and low hills occupied for about 0.10 and 0.24 respectively. It was found by comparison that the evapotranspiration different between landform types was not significantly. It was due to the undulating terrain and the smaller slope and altitude of the study area. Low hills were the highest for about 1.33 mm/day or more, while it is smaller in micro-heights area. There is a strong correlation between evapotranspiration and vegetation cover in different kind of landforms.

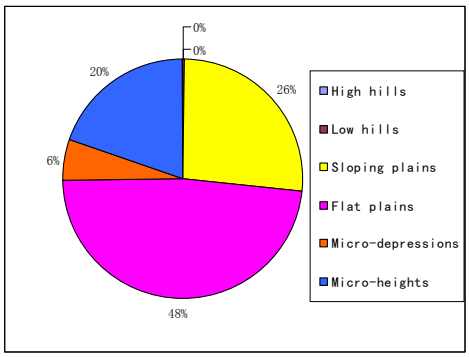

Figure 6. Proportion of different landforms area

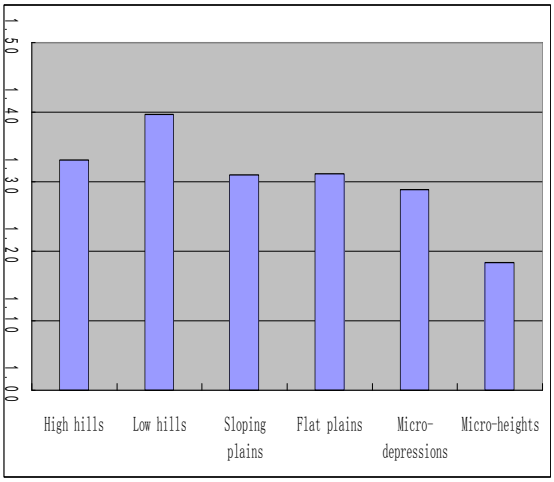

Figure 7. Mean daily evapotranspiration for different landforms

5. CONCLUSION

Elevation and slope-aspect data were incorporated into SEBAL in this study. This substantially improved estimates of ET and other energy balance components in mountainous terrain. The

maximum value of evapotranspiration appeared in the water body, while the minimum value occurs in area of saline and unused land which have sparse vegetation. It always has high evapotranspiration value in farmland areas for higher vegetation coverage. It was found by comparison that the evapotranspiration different between landform types was not significantly due to the undulating terrain and the smaller slope and altitude of the study area.

ACKNOWLEDGES

The author are grateful for the support from Natural Science Foundation of China (41171334，41071278) , Ecological Innovation & Breeding Project (Y254021031，355031061) and USDA NIFA project (2010-34263-21075) , Special research topics of Shandong province information technology and industrialization (2012EI032).

REFERENCE

1. Jiang Le, Islam Shafiqul, Guo Wei et al. A satellite-based daily actual evapotranspiration estimation algorithm over South Florida. *Global and Planetary Change*, 2009, 67(1/2): 62-77.

2. Choudhury B J, DiGirolamo N E. A biophysical process-based estimate of global land surface evaporation using satellite and ancillary data: I. Model description and comparison with observations. *Journal of Hydrology*, 1998, 205(3/4): 164-185.

3. Bastiaanssen W G M, Molden D J, Makin I W. Remote sensing for irrigated agriculture: Examples from research and possible applications. *Agricultural Water Management*, 2000, 46(2): 137-155.

4. Bast iaan ssen W G M. SE BAL-based Sensible and Latent Heat Fluxes in the Irrigated Gediz Basin, Turkey [J] . *Journal of Hydrology,* 2000, 229: 87-100.

5. Bastiaanssen W G M , M enent i M, Feddes R A, et al . A Remote Sensing Surf ace Energy Bal an ce Algorithm for Land (SEBAL)1. Formulation [J] . *Journal of Hydrology,* 1998,212-213: 198-212.

6. Bastiaanssen W G M , Pelgrum H, Wang J , e t al . A Remote Sensing Surface Energy Balance Algorithm for Land (SEBAL)2. Validation [J] . *Journal of Hydrology,* 1998, 212-213:213-229.

7. Pan Z Q, Liu G H. Evapotranspiration Research of Yellow River Delta Using Remote Sensing Method [J] . *Geo-in format ion Science,* 2003, 3: 91-96.

8. Liebe H J, Hufford G A, Cot t on M. C. Propagation Modeling of Moist Air and Suspended Wat er/ ice Part icl es at Frequencies Below 1000GH z [Z] . *AGAED 52nd Special Meeting of the Electromagnetic Waue Propagation Pand,* 1993, 3: 1-10.

9. Wu C D, Cheng C C, Lo H C et al. Application of SEBAL and Markov models for future stream flow simulation through remote sensing. *Water Resources Management,* 2010, 24(14): 3773-3797.